Microwave-Assisted Synthesis of Water Soluble ZnSe@ZnS Quantum Dots

Sonia J. Bailon-Ruiz[*], Oscar Perales-Perez[*, **] and Surinder P. Singh[**]

[*] Department of Chemistry, University of Puerto Rico, Mayaguez, sonia.bailon@uprm.edu
[**] Department of Engineering Science & Materials, University of Puerto Rico, Mayaguez, oscarjuan.perales@upr.edu, surinder.singh@upr.edu

ABSTRACT

Water-soluble quantum dots of ZnSe@ZnS were synthesized under microwave irradiation at different temperatures in presence of thioglycolic acid (TGA). X-ray diffraction analyses suggested the development of a ZnSe-ZnS structure and an average crystallite size of 4.1 ± 0.4 nm. High-resolution transmission electron microscopy evidenced the formation of spherical nanocrystals. UV-vis analyses of nanocrystals synthesized at 120°C clearly showed the exciton peak centered at 290 nm. The corresponding photoluminescence spectrum evidenced a sharp and intense emission peak (FWHM ~ 32 nm) centered at 380 nm; the emission peak was broadened (FWHM ~ 47 nm) when the synthesis temperature was increased up to 140 °C. The strong emission in the nanocrystals synthesized at 120°C was attributed to the suitable development of the ZnS shell onto the ZnSe core.

Keywords: quantum dots, nanocrystals, semiconductors, microwave-assisted synthesis.

1 INTRODUCTION

Semiconductors nanocrystals, also known as quantum dots (QD's), are the focus of an intensive research because of the capability of tuning their optical properties by controlling crystal-size, composition or shape at the nanoscale. Compared to organic dyes, QDs are characterized by their narrow emission spectra, large quantum yield, chemical stability against photo-bleaching and surface functionality. These features make QDs dots very promising candidates for photodynamic therapy agents, biomarkers and also as components in optoelectronics devices. Regarding the use of "traditional" CdSe-based QDs for biomedical applications, their potential cytotoxicity makes necessary the search of alternative and less-toxic Cd-free nanomaterials [1-3]. Among different Zn-based QDs, highly luminescent ZnSe nanocrystals have been synthesized from organometallic diethylzinc precursor in a trioctylphospine oxide (TOPO)-hexadecylamine (HAD) mixture [4]. However, the precursor salts are extremely toxic, expensive and pyrophoric. ZnSe QDs exhibiting a hydrophobic surface have also been synthesized from precursor ZnO at temperatures as high as 350°C [5]. As an attempt to enhance the photoluminescence (PL) intensity and the quantum yield even more, the formation of QDs consisting of a ZnS-shell surrounding a ZnSe-core has been suggested [6]. In this regard, the synthesis of core-shell ZnSe@ZnS QD's in presence of thiols becomes a very promising alternative route to organometallic reactions due to: (i) high synthesis temperatures are not necessary; (ii) the precursors salts are not dangerous and easy to handle; (iii) the core-shell arrangement allows the achievement of an excellent photo-stability of the water-soluble nanocrystals; and, (iv) easy surface functionalization in aqueous media [7,8]. Microwave-assisted synthesis is an attractive method to produce the targeted core-shell arrangements because of its high heating rate and homogeneous heating capability which promotes the formation of crystalline and high-optical quality QD's [8,9]. This method is also energy efficient as compared to conventional hydrothermal approaches [9]. Under these considerations, the present study addressed the systematic evaluation of the microwave-assisted synthesis of water-soluble ZnSe@ZnS quantum dots using thioglycolic acid (TGA) as the source of sulfide ions.

2 MATERIALS AND METHODS

2.1 Materials

Zinc chloride (99.999% trace metals basis), elemental selenium powder (99.99% trace metals basis), sodium bisulfite (> 98%) and Thioglycolic acid (TGA, ≥ 98.0 %) were purchased from SIGMA-ALDRICH. All materials were used without further purification.

2.2 Synthesis of ZnSe@ZnS QDs

Selenide ions solution was prepared by reducing elemental selenium powder with sodium bisulfite. Zinc and selenium solutions were mixed in a microwave digestion vessel in presence of TGA at pH 7.0 and heated for one hour at 100°C, 120°C and 140°C. The molar ratio of Zn/TGA/Se was optimized and fixed at 1/ 4.8 / 0.04 for all tests. Once the reaction was completed, the obtained suspension was cooled down to room temperature. The formed nanocrystals were coagulated with 2-propanol, centrifuged and resuspended in deionized water.

2.3 Characterization Techniques

Samples were structurally characterized by X-ray diffraction (XRD) in a Siemens Powder Diffractometer D5000 using Cu-Kα radiation. The high-resolution TEM (HRTEM) study was performed in a FEI-TITAN unit operated at 200 KV. UV-vis absorption measurements were carried out using a Beckman DU 800 Spectrophotometer. A Shimadzu RF-5301 spectrofluorometer with spectral bandwith 5-5 and a 150W xenon lamp was used to collect the photoluminescence (PL) spectra at room temperature. Inductive Coupled Plasma Mass Spectrometer (ICP-MS) Agilent 7500ce was used to confirm the presence of Zn and Se in synthesized QD's.

3 RESULTS AND DISCUSSION

3.1 Structural and Morphological Characterization

Figure 1 shows the XRD pattern of the powder synthesized in presence of TGA at 120°C and pH 7.0. The as-synthesized sample exhibited a cubic structure of zinc blende. No diffraction peaks for isolated ZnSe (JCPDS N° 80-0021) or ZnS (JCPDS N° 77-2100) were observed, which indicates the presence of only one type of crystalline phase. Qian *et al*., [9] suggested that the location of the XRD lines between the ones corresponding to pure ZnSe and ZnS phases should be attributed to the formation of ZnSe-ZnS core-shell like structure. Xie *et al*. mentioned that the thickness of the shell could also affect the position of the diffraction peaks [10]. In turn, the broadening of the diffraction peaks suggested the presence of very small nanocrystals; the average crystallite size, estimated according to the Debye-Scherrer's relationship, was 4.1 ± 0.4 nm. The corresponding lattice parameter "*a*" was estimated at 0.543 nm. This value is within the 0.567 nm (ZnSe) - 0.538 nm (ZnS) range.

The formation of nanosize crystals can be explained by the extremely fast nucleation rate during the formation of the ZnSe core favored by the direct reaction between available Zn and selenide species. The subsequent formation of the ZnS shell would have taken place by reaction of the excess of Zn ions with sulfide species generated by the thermal decomposition of the TGA thiol. According to Qian *et al*., [9] the presence of atmospheric oxygen in the reaction vessel used during the microwave irradiation would have enhanced the decomposition of the HS^- groups in TGA to sulfide anions. Furthermore, the adsorption of non-reacted thiol species onto the QDs surface should favor the establishment of a net negative surface charge that should have prevented the nanocrystals from aggregation [7, 9].

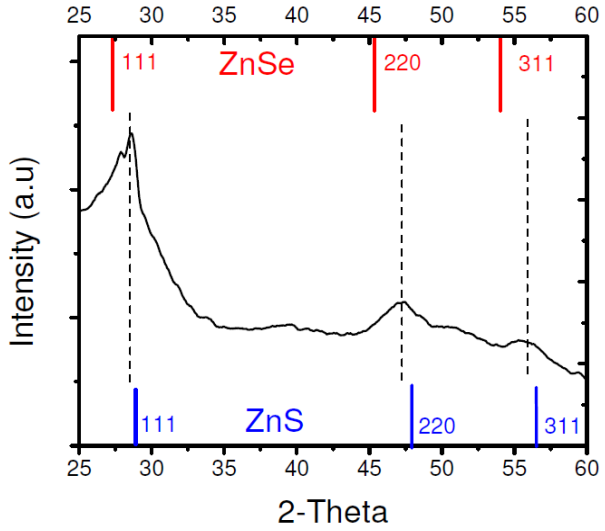

Figure 1: XRD pattern of ZnSe@ZnS powder synthesized in presence of TGA. The pH value and reaction temperature were 7.0 and 120°C, respectively. Expected diffraction lines for pure ZnSe and ZnS phases are also shown.

The HRTEM image of figure 2 corresponds to ZnSe@ZnS core-shell QDs. The image evidenced the crystallinity of the QDs even at such a small size (around 4nm). The lattice spacing for the nanocrystal in the inset was about 0.31 nm, corresponding to the (111) plane of cubic ZnSe core (JCPDS N° 80-0021).

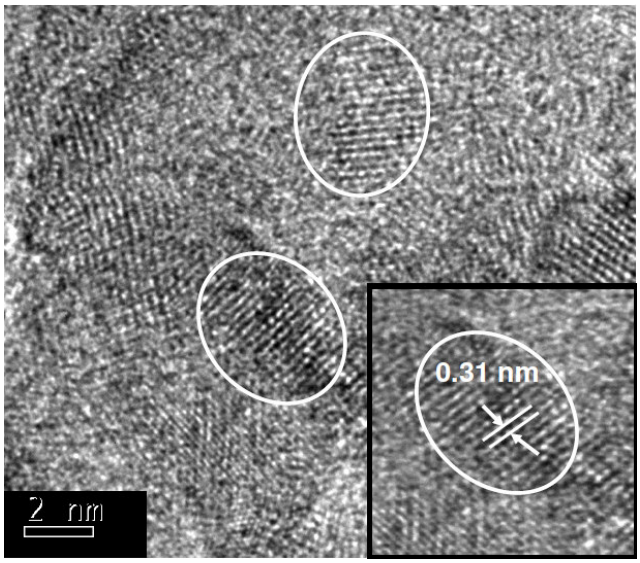

Figure 2: HRTEM image of ZnSe@ZnS quantum dots synthesized at 120°C and pH 7.0.

3.2 UV-Vis and Photoluminescence Measurements.

Figure 3 shows the UV-Vis absorption spectra of ZnSe@ZnS nanocrystals synthesized at different reaction temperatures. The promotion of crystal growth by increasing of the reaction temperature was suggested by the red-shift of the corresponding exciton peak.

The optical band gap energy (E_g) for each sample was estimated from Tauc's relationship and plotting the variation of $(\alpha h\upsilon)^2$ with $h\upsilon$. Here, $h\nu$ and α are the photon energy and the absorption coefficient, respectively, and are obtained from the corresponding UV-vis absorption spectra [11]. As figure 4 shows, the intercept of the linear portion of the plot with the energy axis gives the corresponding band gap value. Accordingly, the band gap for the nanocrystals synthesized at 100°C, 120°C and 140°C were estimated at 4.82 eV, 4.80 eV and 4.06 eV, respectively. These E_g values are larger than the one for bulk ZnSe (2.7 eV) and ZnS (3.67 ev) [6,9], which is indicative of the quantum confinement effect.

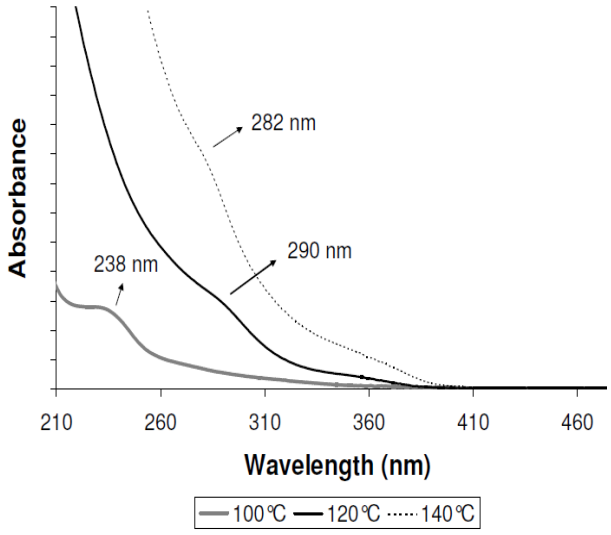

Figure 3: Absorption spectra of core-shell ZnSe@ZnS quantum dots synthesized at pH 7.0 and various reaction temperatures.

The room-temperature PL spectra of QDs synthesized at various reaction temperatures and Zn/TGA/Se molar ratio of 1/ 4.8 / 0.04, are shown in figure 5. The spectra were recorded using an excitation wavelength of 300nm.

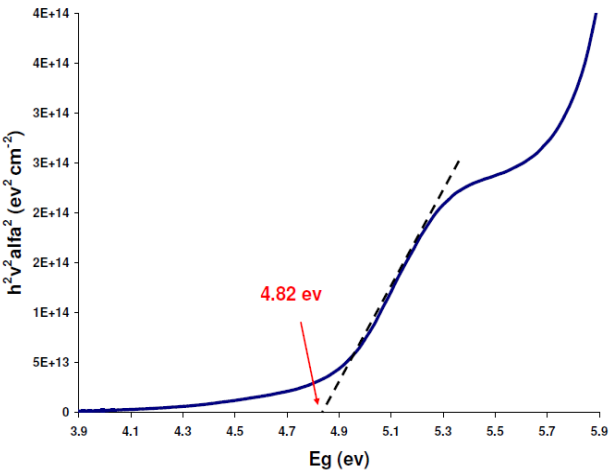

Figure 4: Determination of the band gap value for core-shell ZnSe@ZnS quantum dots synthesized at 100°C and pH 7.

As seen, an intense band edge emission with a FWHM of 32 nm became evident at 380nm in the PL spectrum of the sample synthesized at 120°C. The formation of the ZnS shell onto the ZnSe core should have improved the luminescent properties of these nanocrystals in comparison to bare ZnSe [7]. The luminescence intensity went down and the emission peak broadened when QD's were synthesized at 140°C. This drop in photoluminescence can be attributed to a much larger coverage of the ZnSe by ZnS [12]. Dabbousi *et al.* mentioned that the growth of ZnS shell onto the ZnSe core could be coherent at low coverage. However, as far as the thickness of the shell is increased, the strain due to the lattice mismatch between the core and the shell would lead to the formation of dislocations and low-angle grain boundaries, relaxing the structure and causing the ZnS growth to proceed incoherently. These defects would promote non-radiative recombinations within the ZnS shell that caused the observed decrease in the luminescence intensity [12]. On the other hand, the quenching in photoluminescence observed in QDs' synthesized at 100°C can be attributed to an incomplete or inadequate development of the ZnS layer due to the poor generation of free sulfide ions at such a low temperature. Moreover, as suggested by Deng *et al.,* the presence of structural defects in tinier crystals could also be involved with the observed drop in luminescence [7].

UV-Vis and PL measurements evidenced the Stokes' shift between the absorption and emission maximum. The magnitude of the Stoke's shift for samples synthesized at 100°C, 120°C and 140°C were 150 nm, 90 nm and 140 nm, respectively. Stoke's shift can be a consequence of the increased delocalization of the electron and the consequent lowering of the corresponding excited state energy, both caused by the formation of the ZnS shell [12]. The

dependence of the magnitude of the Stoke's shift with the thickness of ZnS layer has also been reported for CdSe@ZnS QDs [12].

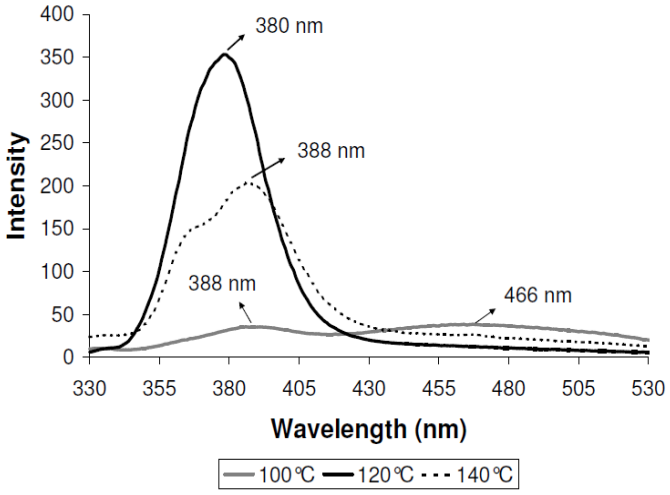

Figure 5: Photoluminescence spectra of core-shell ZnSe@ZnS quantum dots synthesized at 100°C, 120°C and 140°C. The excitation wavelength was 300 nm.

4 CONCLUSIONS

Crystalline and water-soluble quantum dots have been synthesized under microwave irradiation. X-ray diffraction and optical characterization suggested the formation of a ZnSe@ZnS core-shell structure. Luminescence of these core-shell nanocrystals was strongly dependent on the synthesis temperature; the emission intensity reached a maximum when QDs' were synthesized at 120°C. This strong emission was attributed to the adequate formation of a ZnS shell on the ZnSe core.

5 ACKNOWLEDGEMENTS

The support from Drs. E. Melendez and F. Roman, Faculty at the department of Chemistry-UPRM, is acknowledged. The authors also thank to Dr. P. M. Voyles, Faculty at the Department of Materials Science and Engineering-University of Wisconsin at Madison, and Yarilyn Cedeño, doctoral student at UPRM, for their assistance with TEM analyses. This material is based upon work supported by The National Science Foundation under Grant No. HRD 0833112 (CREST program).

REFERENCES

[1] N. Pradhan, and X. Peng, *J. Am. Chem. Soc.* 129, 3339. 2007.

[2] P. Juzenas, W. Chei, Y. Sun, M. Neto, R. Generalov, N. Generalova, and I. Christensen, *Adv. Drug Deliv*. Rev. 60, 1601-1602. 2008.

[3] W. W. Yu, E. Chang, R. Drezek, and V. L. Colvin, *Biochem. Biophys. Res. Commun*. 348, 781-782. 2006.

[4] M. A. Hines and P. Guyot-Sionnest, *J. Phys. Chem. B.* 102, 3655-3657. 1998.

[5] L. S. Li, N. Pradhan, Y. J. Wang and X. G. Peng, *Nano Lett*. 4, 2261-2264. 2005.

[6] C. Hwang and I. Cho, *Bull. Korean Chem. Soc.* 26 (11), 1776-1779. 2005.

[7] Z. Deng, F. L. Lie, S. Shen, I. Ghosh, M. Mansuripur and A. J. Muscat, *Langmuir*. 25, 434-435. 2009.

[8] S. J. Bailon-Ruiz, O. Perales-Perez, S. P. Singh and P. M. Voyles, *Mater. Res. Soc. Symp. Proc.* 1207 (N10-61), 1-2. 2010.

[9] H. Qian, X. Qiu, L. Li and J. Ren, *J. Phys. Chem.* B110, 9034-9037. 2006.

[10] R. Xie, U. Kolb, J. Li, T. Basche and A. Mews, *J. Amer. Chem. Society*. 127,7484. 2005.

[11] J. Tauc, "Amorphous and liquid semiconductors", New York , 159, 1974.

[12]. B.O. Dabbousi, J. Rodriguez-Viejo, F.V. Mikulec, J.R. Heine, H. Mattoussi, R. Ober, K. F. Jensen, and M. G. Bawendi, *J. Phys. Chem.* B101, 9473. 1997.